

Synthesis of a gold nanoparticle dimer plasmonic resonator through two-phase-mediated functionalization

This content has been downloaded from IOPscience. Please scroll down to see the full text.

2008 Nanotechnology 19 435605

(<http://iopscience.iop.org/0957-4484/19/43/435605>)

View [the table of contents for this issue](#), or go to the [journal homepage](#) for more

Download details:

IP Address: 136.152.209.32

This content was downloaded on 29/06/2015 at 17:44

Please note that [terms and conditions apply](#).

Synthesis of a gold nanoparticle dimer plasmonic resonator through two-phase-mediated functionalization

Tae-Jin Yim¹, Yuan Wang¹ and Xiang Zhang^{1,2,3}

¹ NSF Nanoscale Science and Engineering Center (NSEC), University of California, Berkeley, CA 94720-1740, USA

² Materials Sciences Division, Lawrence Berkeley National Laboratory, Berkeley, CA 94720, USA

E-mail: xiang@berkeley.edu

Received 6 June 2008, in final form 7 August 2008

Published 22 September 2008

Online at stacks.iop.org/Nano/19/435605

Abstract

We report that Au nanoparticles, ligand-exchanged with a thiol ligand at the liquid–liquid interface, were dimerized using an *N,N'*-diisopropylcarbodiimide-mediated amide bond formation. This dimerization of 60 nm sized Au nanoparticles achieved 24% overall yield and was visually confirmed by transmission electron microscopy as well as by scanning electron microscopy images. The resultant electromagnetic field enhancement of a single Au nanoparticle dimer was proven by dark field spectroscopy which, in turn, made the Au nanoparticle dimer suitable for molecular sensing applications, such as in surface enhanced Raman spectroscopy. Our dimerization method demonstrated that the synthesis of Au nanoparticle dimers with a high yield and enhanced optical properties of the dimers were possible. Our methodology also has good prospects as regards the formation of nanoscale building blocks.

(Some figures in this article are in colour only in the electronic version)

1. Introduction

Inorganic nanoparticles have been examined for optoelectronics [1], nanoelectronics [2], chemical sensing [3], nanomedicine [4], and molecular imaging [5]. Au and Ag nanoparticle plasmonic resonators, in particular, have received significant attention. Nanoparticle assemblies, which are dimerized Au and Ag nanoparticles, have been found to have interesting resonant properties that arise from the hybridization of the individual particles' resonance. The dimerization of the nanoparticles provides a new way to design the collective resonances at the desired frequencies that are often needed for molecular sensing tools, such as surface enhanced Raman spectroscopy (SERS) [6–8]. It should be noted that electromagnetic (EM) field enhancements from large aggregates and arrays of the Au nanoparticles exist, too. However, contrary to the aggregates and arrays, it is expected that the smaller-sized Au nanoparticle dimers possess good

control of production and advantage for *in vitro* and *in vivo* studies as well as consistent properties including EM field enhancement. Various strategies [9–14] to form nanoparticle dimers include: the formation of Au nanoparticle dimers through functionalization using a solid bead support [10], heterodimeric nanostructures with particle specific functionalization [11], FePt–Au heterodimers for dual mode detection with *in vitro* magnetic resonance imaging (MRI) [12], homo- and hetero-Au nanoparticle dimers through functionalization on two dimensional solid surface [13], and DNA based Au nanoparticle assembly [14]. Additionally, recent theoretical [15] and experimental [7] studies of the optical properties of nanoparticle dimers have been reported. However, in order to develop the nanoparticle dimer plasmonic resonator, there is still the challenge of synthesizing nanoparticle dimers in a manner that satisfies both reliable synthesis with a high yield and desired optical properties. In order to ensure for a careful design of nanoparticle dimers, having a gap, rather than direct contact between the two nanoparticles, is required to form a

³ Author to whom any correspondence should be addressed.

highly confined and enhanced local EM field [16–18]. Both the resonance frequency and field strength can also be tuned by the distance of the dielectric layer (gap) between the two nanoparticles [17].

Here, we report a new method that is able to produce Au nanoparticle dimers through the ‘ligand-exchange’ of the Au nanoparticles at liquid–liquid interfaces, resulting in a high yield of nanoparticle dimers with enhanced optical property as compared to nanoparticle monomers. The liquid–liquid interface has been applied to the synthesis of nanoparticles [19], stabilization of nanoparticles at the interface [20], and the formation of nanoparticles assembly [21]. The emulsion of the immiscible toluene–water interface by sonication provides the self-assembly monolayer (SAM) layered nanoparticles with great interfacial contact, but with less accessibility to aqueous thiol molecules than a single aqueous phase. This lesser accessibility to aqueous thiol molecules by the toluene–water interface is useful in order to avoid replacing all SAM on the nanoparticles with aqueous thiol molecules within a short period of time. Therefore, we reasoned that the ligand-exchange of SAM layered Au nanoparticles can be achieved by, for a short time exposing them, to aqueous thiol molecules at the toluene–water interface with sonication.

2. Materials and methods

2.1. Materials

Au nanoparticles were purchased from BBI International (Ted Pella, Redding, CA), and all of the other chemicals, including 6-mercapto-1-hexanol, tiopronin, 1-nonanethiol, ethylenediamine, and *N,N'*-diisopropylcarbodiimide (DIC), were purchased from Sigma-Aldrich (St Louis, MO). All other materials were used as received without any further purification.

2.2. Formation of the dimers through two-phase ligand-exchange

For the synthesis of the dimers, 7.8×10^{10} particles of citrate-stabilized Au nanoparticles (60 nm in diameter) in water were centrifuged to remove the water content, were redispersed in ethanol by sonication, and ethanol was removed by centrifugation. Next, in order to form a mixed SAM layer on the Au nanoparticles, Au nanoparticles were incubated overnight with 1 ml of 2.25 mM mixed thiol ligands in ethanol at a 2:1 loading molar ratio of 1-nonanethiol to 1-mercapto-6-hexanol. After removing ethanol by centrifugation, the SAM layered Au nanoparticles were dispersed in 150 μ l of toluene by the process of sonication, and this was followed by adding 850 μ l of 20 mM tiopronin in water to the SAM layered Au nanoparticles. The sample was then sonicated for 10 min in order to form a toluene–water interface allowing for ligand-exchange. To wash the unbound tiopronin and to obtain the ligand-exchanged Au nanoparticles, 0.5 ml of tetrahydrofuran (THF) was added to the reaction mixture, and this was centrifuged to discard the supernatant. The ligand-exchanged Au nanoparticles were washed again with THF,

and then redispersed in *N,N'*-dimethylformamide (DMF). For dimerization, 40 μ l of 10 mM DIC was added to the ligand-exchanged Au nanoparticles in 3 ml of DMF, and the reaction mixture was incubated for 3 h, during which time 1 ml of 10 mM ethylenediamine in DMF was added dropwise to them for the initial 20 min [22]. Finally, the mixture was centrifuged to discard the supernatant, and the particles were washed with methanol and dispersed in methanol for transmission electron microscopy (TEM) and scanning electron microscopy (SEM) analyses.

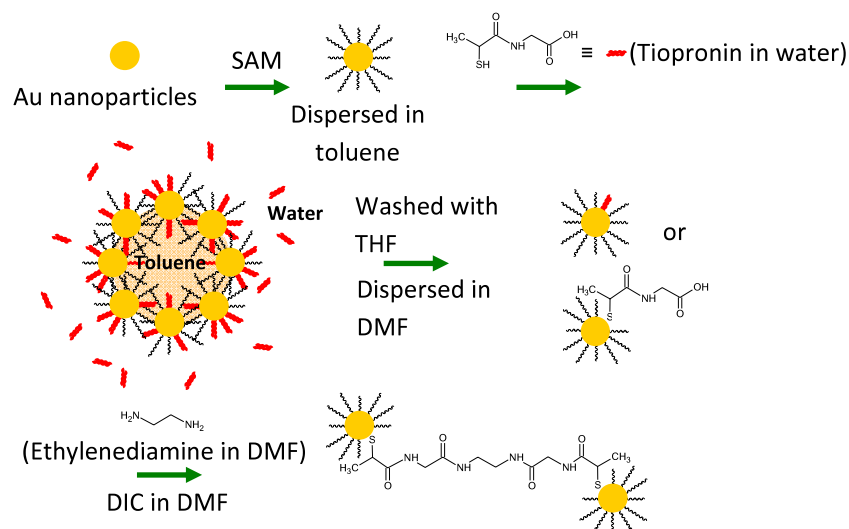
2.3. Control through one-phase ligand-exchange

Control experiments were performed with both citrate-stabilized (as received) and SAM layered (same protocol as above) Au nanoparticles (60 nm in diameter). In regard to ligand-exchange of Au nanoparticles, both Au nanoparticles were dispersed with 20 mM tiopronin in water to generate carboxylic groups on Au nanoparticles using sonication for 10 min. To wash the unbound tiopronin, 0.5 ml of tetrahydrofuran (THF) was added to the reaction mixture, and this was centrifuged to discard the supernatant. The ligand-exchanged Au nanoparticles were washed again with THF, and then redispersed in DMF. 40 μ l of 10 mM DIC was separately added to the both ligand-exchanged Au nanoparticles in the 3 ml of DMF and this was incubated for 3 h, when 1 ml of 10 mM ethylenediamine in DMF was added in a dropwise manner for an initial 20 min. Finally, each mixture was centrifuged to remove the supernatant, and the particles were washed with methanol and dispersed in methanol for SEM analysis.

2.4. Dark field spectroscopy

To place nanoparticles on a support for optical property measurement, a poly(methylmethacrylate) (PMMA) layer on top of an ITO (indium tin oxide, \sim 5 nm in thickness)-coated quartz plate was patterned by an e-beam lithography (circular-shaped patterns of \sim 140 nm in diameter were located 4 μ m apart, in horizontal and vertical axes). By incubating the well with a dispersed sample in methanol, both single monomers and single dimers of Au nanoparticles were placed on an ITO-coated quartz plate. After removing the PMMA layer with acetone, the SEM image of the sample array was taken to mark the position of the single monomers and single dimers, respectively.

A dark field spectroscopy was used for the optical confirmation of the Au nanoparticle assembly and this was performed with an Axiovert 200 inverted microscope setup (Carl Zeiss MicroImaging Inc., Thornwood, NY) equipped with a dark field mirror block, and a dark field objective (50 \times , NA = 0.5). The sample was illuminated by a 100 W tungsten lamp. The scattered light was analyzed by a Triax spectrometer (HORIBA Jobin Yvon, Edison, NJ) equipped with a liquid nitrogen cooled charge-coupled device (CCD) detector. A spectrum was obtained by measuring the signals from the single particles in the air, subtracting the background signals taken nearby from the single particle signals, and normalized by the intensity of incident light.



Scheme 1. The procedure of the assembly of Au nanoparticle dimers (the SAM layer: 1-nonanethiol (-----), and 1-mercapto-6-hexanol (—)), and ligand-exchange: tiopronin (---)).

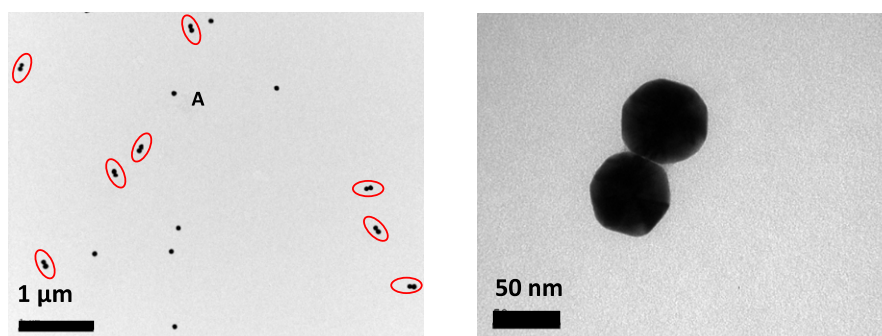


Figure 1. TEM images of assembled Au nanoparticle dimers (marked on the left, separation of the dimers: less than 2 nm, and highlighted on the right) through ligand-exchange for 10 min and unreacted Au nanoparticle monomers.

2.5. Simulation method

The 3D simulations were performed using Drude model in a commercial FDTD (finite-difference time-domain) software (CST Microwave Studio, CST, Framingham, MA) under a linearly polarized plane wave illumination with an E-field amplitude of 1 V m^{-1} . The simulated monomer and dimer were composed of gold nanoparticles with a diameter of 60 nm. The gap of the dimer between the nanoparticles was 2 nm. The dielectric constant of gold was taken from a literature [23].

3. Results and discussion

The Au nanoparticle dimers were produced through ligand-exchange of a nanoparticle surface using a toluene–water interface and a short sonication time, while the aggregation was dominantly formed when the SAM layered nanoparticles were ligand-exchanged in the single aqueous phase. As depicted in scheme 1, the mixture of the 1-nonanethiol and the 1-mercapto-6-hexanol (MCH) in ethanol were first chemisorbed on Au nanoparticles overnight, resulting in the formation of the SAM on the whole surface of the Au nanoparticles. The MCH, which is a shorter ligand than the 1-nonanethiol, is known to

create a relatively less stable SAM, therefore the mixed thiol ligands (with a 2:1 loading molar ratio of 1-nonanethiol to MCH) provide defect sites where the SAM molecules are to be replaced by aqueous tiopronin [24]. Consequently, the SAM defects on the Au nanoparticles were ligand-exchanged with carboxylic acids (tiopronin) in water by sonication for 10 min. The ligand-exchanged Au nanoparticles were well dispersed in *N,N'*-dimethylformamide (DMF) and then dimerized with an *N,N'*-diisopropylcarbodiimide (DIC)-mediated amide bond formation. The gap size in a dimer should be less than 2 nm when ethylenediamine is used as a linker. A further increase in the particle–particle distance can be achieved by simply choosing longer diamine compounds.

The resultant assembly of the Au nanoparticles was visually confirmed by a transmission electron microscopy (TEM) (figure 1). As illustrated in these images, there are numerous assembled dimers and some unreacted monomers, but there are few higher-ordered assemblies (clusters). The overall dimerization yield was estimated utilizing the method by Shumaker-Parry and co-workers [13]. Briefly, it was determined by counting at least 500 of the nanoparticles from the 25 TEM images that were randomly taken. The overall

yield of the dimerization was ca 24%. This efficiency is quite high since our TEM samples contain *all* of the particles, without any separation from the initial step. Even though Shumaker-Parry and co-workers produced 46% yield in case of 41 nm sized Au nanoparticles [13], the washed particle number in the initial step was not counted and the yield is dependent on the nanoparticle size, and therefore it is difficult to compare it with our result. Our overall yield was similar when the concentration of aqueous tiopronin was over 2 mM. The dimerization through ligand-exchange under the same conditions, with the exception of the shorter reaction time (2 min) produced a ca 21% overall yield, but higher-ordered clusters were generated, in fact, twice as many as seen in the ligand-exchange assisted by sonication for 10 min due to the hydrophobic nanoparticle surface. Likewise, the ligand-exchange for a longer period of time (30 min) produced a ca 27% overall yield, but higher-ordered clusters were also generated, three times as many as observed in the ligand-exchange with sonication for 10 min. For a size effect on the dimerization, the dimerization of particles smaller than 60 nm under the same conditions produced a lot of clusters compared to those of 60 nm particles. In contrast to smaller particles (less than 20 nm in diameter), the dimerization of particles larger than 60 nm under the same conditions produced almost same overall yield and few clusters as those of 60 nm particles. According to a previous report, nanoparticles are mobile size-dependently at the toluene–water interface [25], thus the ligand-exchange in our case must have occurred at multiple and random sites on the Au nanoparticle, and were time-dependently controlled by the two-phase system. The Au nanoparticle sample (60 nm) that is prepared using sonication for 10 min is more beneficial to separate dimers since the sample is mainly composed of monomers and dimers. Although our method can control the dimerization of larger particles better than that of smaller-sized nanoparticles, the size of particles fits well with the dimerization of the larger nanoparticles (typically 40–100 nm) which have higher local field enhancement at optimum surface plasmon resonance [26].

Control experiments were conducted in order to demonstrate the advantage of the SAM layer and of two-phase mediated ligand-exchange. The first control experiment was that both citrate-stabilized Au nanoparticles ligand-exchanged with 20 mM tiopronin in single aqueous phase and the citrate-stabilized (unfunctionalized) Au nanoparticles proceeded to dimerization through DIC-mediated amide bond formation. Both of the Au nanoparticles produced a great deal of clusters due to the existence of carboxylic groups which stemmed from either citrate molecules or tiopronin molecules on the nanoparticle surface ((a) and (b) in figure 2). This result indicates that the concentration of tiopronin cannot be dialed in the single aqueous phase, and that our alkyl- and hydroxyl-terminated SAM layer can be advantageous in controlling the number of carboxylic reaction sites in the ligand-exchange step.

The second control experiment was performed in order to confirm the significance of the Au nanoparticle dimerization through a two-phase mediated ligand-exchange, the whole surfaces of the SAM layered Au nanoparticles as well as

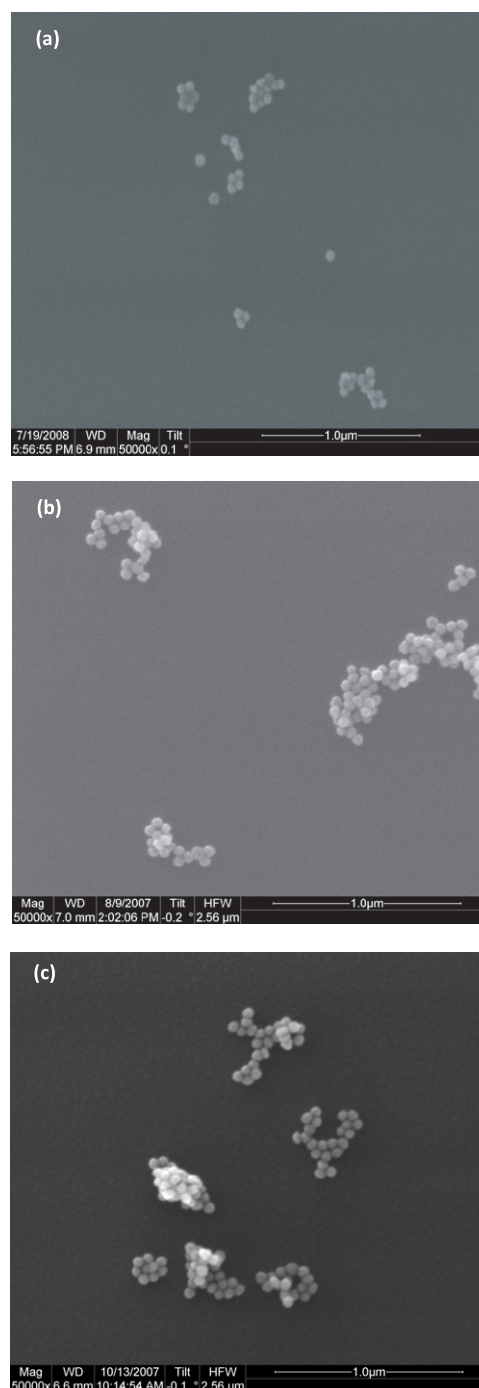


Figure 2. SEM images of control experiments, (a) citrate-stabilized Au nanoparticles, (b) citrate-stabilized Au nanoparticles ligand-exchanged with tiopronin in single aqueous phase, and (c) SAM layered Au nanoparticles ligand-exchanged with tiopronin in single aqueous phase.

the citrate-stabilized Au nanoparticles (the same as above) were ligand-exchanged with tiopronin in water. The amide bond formation of both control samples resulted in heavy aggregations of nanoparticles ((b) and (c) in figure 2). More importantly, this control experiment demonstrates that the ligand-exchange of the Au nanoparticles obtained by our toluene–water interface methodology is critical to produce Au

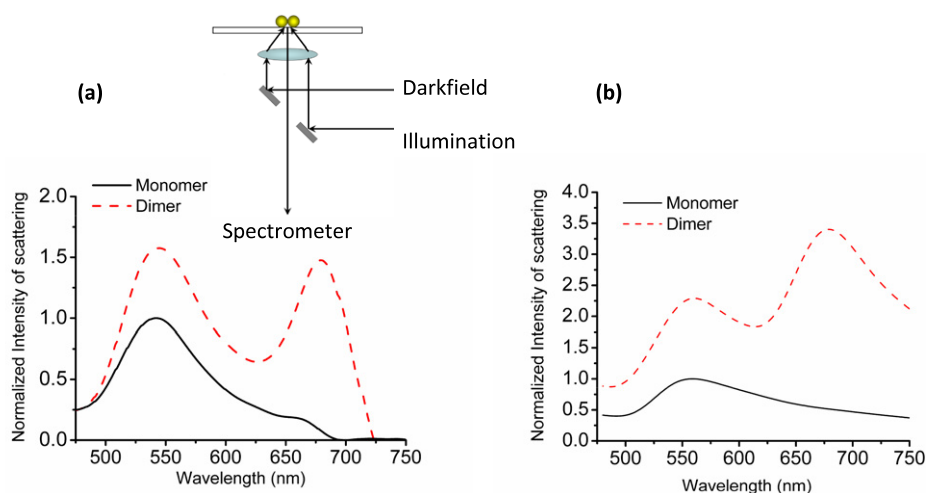


Figure 3. (a) The dark field scattering of a single Au nanoparticle monomer and a single dimer (the isolated monomers and dimers were placed on an indium tin oxide (ITO)-coated quartz plate prepared by e-beam lithography) and the dark field spectroscopy setup. (b) A simulation of the scattering intensity of a single monomer and a single dimer.

nanoparticle dimers with a high yield, and that whole ligand-exchange leads to the aggregation of Au nanoparticles, whether or not a SAM layer on the Au nanoparticles exists.

The formation of the Au nanoparticle dimers can also be verified by EM field enhancement. The EM field enhancement has been supported by either resonance scattering for nanosensing [27] or absorption for therapeutics [28]. It was reported that interacting plasmons promoted the absorption mechanism of island structure composed of the ultrathin Au thin film (≤ 10 nm) [29]. Additionally, it was expected that larger nanoparticles would be suitable for light scattering, while intermediate-sized nanoparticles would be good for photoabsorption [30]. Therefore, in our study, the scattering of both a single monomer and a single dimer of the Au nanoparticle was measured in air at far field using dark field spectroscopy with reflected illumination. Even though particle to particle spectral variation due to the difference in the nanoparticle's morphology and gap size was observed, the general difference between the single monomer and single dimer was apparent, as follows. In the spectra taken from the single Au nanoparticle monomers, one plasmon resonance peak at 540 nm is observed (figure 3(a)). In regard to the single Au nanoparticle dimers, two resonance peaks are found. The longer wavelength resonance peak at 680 nm originates from the excitation of the hybridized surface plasmon modes that are parallel to the long axis of the dimer with a separation of less than 2 nm, and these always have a characteristic red shift from the monomer plasmon resonance. The shorter wavelength resonance peak of the dimers is owing to the excitation of the hybridized surface plasmon modes that are perpendicular to the long axis of the dimer [6, 31]. All of the single monomers and single dimers measured in our experiment were found to have much stronger dark field scattering intensity from a single dimer than that seen from a single monomer, at both 540 and 680 nm, and this is approximately correspondent to that of our numerical simulation result. Figure 3(b) shows the wavelength dependence for the intensity of the scattering from

a monomer and a dimer. At both 540 and 680 nm, a much stronger scattering intensity from a single dimer than that from a single monomer was found.

4. Conclusion

In summary, we have demonstrated that the Au nanoparticles were dimerized through ligand-exchange with aqueous thiol molecules at a toluene–water interface. This method was proven to be a simple and reproducible synthesis of Au nanoparticle dimers with a high yield. Furthermore, with the enhanced optical property of the synthesized Au nanoparticle dimers, useful tools such as SERS, can be developed for molecular sensing. For more practical applications, the particle–particle distance needs to be optimized while considering both the EM field enhancement and the space for target molecules. In addition, the partial ligand-exchange of nanoparticles has a great potential for assembly of nanoscale building blocks through utilization of a bottom-up approach.

Acknowledgment

We thank the National Institutes of Health through the NIH Roadmap for Medical Research (PN2 EY018228) for support.

References

- [1] Nelayah J, Kociak M, Stephan O, Garcia de Abajo F J, Tence M, Henrard L, Taverna D, Pastoriza-Santos I, Liz-Marzan L M and Colliex C 2007 *Nat. Phys.* **3** 348–53
- [2] Berry V and Saraf R F 2005 *Angew. Chem. Int. Edn* **44** 6668–73
- [3] Zhao J, Jensen L, Sung J, Zou S, Schatz G C and Van Duyne R P 2007 *J. Am. Chem. Soc.* **129** 7647–56
- [4] Kim J *et al* 2006 *Angew. Chem. Int. Edn* **45** 7754–8
- [5] Gao X, Cui Y, Levenson R M, Chung L W K and Nie S 2004 *Nat. Biotechnol.* **22** 969–76
- [6] Nordlander P, Oubre C, Prodan E, Li K and Stockman M I 2004 *Nano Lett.* **4** 899–903

- [7] Talley C E, Jackson J B, Oubre C, Grady N K, Hollars C W, Lane S M, Huser T R, Nordlander P and Halas N J 2005 *Nano Lett.* **5** 1569–74
- [8] Olk P, Renger J, Haertling T, Wenzel M T and Eng L M 2007 *Nano Lett.* **7** 1736–40
- [9] Brousseau L C III, Novak J P, Marinakos S M and Feldheim D L 1999 *Adv. Mater.* **11** 447–9
- [10] Sung K-M, Mosley D W, Peelle B R, Zhang S and Jacobson J M 2004 *J. Am. Chem. Soc.* **126** 5064–5
- [11] Gu H, Yang Z, Gao J, Chang C K and Xu B 2005 *J. Am. Chem. Soc.* **127** 34–5
- [12] Choi J-S, Jun Y-W, Yeon S-I, Kim H C, Shin J-S and Cheon J 2006 *J. Am. Chem. Soc.* **128** 15982–3
- [13] Sardar R, Heap T B and Shumaker-Parry J S 2007 *J. Am. Chem. Soc.* **129** 5356–7
- [14] Zanchet D, Micheel C M, Parak W J, Gerion D, Williams S C and Alivisatos A P 2002 *J. Phys. Chem. B* **106** 11758–63
- [15] Romero I, Aizpurua J, Bryant G W and de Abajo F J G 2006 *Opt. Express* **14** 9988–99
- [16] Wang H, Levin C J and Halas N J 2005 *J. Am. Chem. Soc.* **127** 14992–3
- [17] Su K H, Wei Q H and Zhang X 2006 *Appl. Phys. Lett.* **88** 063118
- [18] Ringler M *et al* 2007 *Nano Lett.* **7** 2753–7
- [19] Brust M, Walker M, Bethell D, Schiffrin D J and Whyman R 1994 *J. Chem. Soc. Chem. Commun.* **801–2**
- [20] Lin Y, Skaff H, Emrick T, Dinsmore A D and Russell T P 2003 *Science* **299** 226–9
- [21] Glogowski E, Tangirala R, He J, Russell T P and Emrick T 2007 *Nano Lett.* **7** 389–93
- [22] Worden J G, Shaffer A W and Huo Q 2004 *Chem. Commun.* **518–9**
- [23] Lide D R 2001 *CRC Handbook of Chemistry and Physics* (Boca Raton, FL: CRC Press) (Electronic edition)
- [24] Singh C, Ghorai P K, Horsch M A, Jackson A M, Larson R G, Stellacci F and Glotzer S C 2007 *Phys. Rev. Lett.* **99** 226106
- [25] Lin Y, Boeker A, Skaff H, Cookson D, Dinsmore A D, Emrick T and Russell T P 2005 *Langmuir* **21** 191–4
- [26] Nakamura T and Hayashi S 2005 *Japan. J. Appl. Phys.* **44** 6833–7
- [27] Reinhard B M, Sheikholeslami S, Mastroianni A, Alivisatos A P and Liphardt J 2007 *Proc. Natl Acad. Sci. USA* **104** 2667–72
- [28] West J L and Halas N J 2003 *Annu. Rev. Biomed. Eng.* **5** 285–92
- [29] Khriachtchev L, Heikkila L and Kuusela T 2001 *Appl. Phys. Lett.* **78** 1994–6
- [30] Jain P K, Lee K S, El-Sayed I H and El-Sayed M A 2006 *J. Phys. Chem. B* **110** 7238–48
- [31] Wang H and Halas N J 2006 *Nano Lett.* **6** 2945–8